Mixed-Valence Transition Metal Thiophosphates: $AuNb_4P_2S_{20}$

Sung-Jin Kim,*,† Sunah Yim,† Eun-Young Goh,† Haeyong Kang,‡ Woun Kang,‡ and Dongwoon Jung*,§

Departments of Chemistry and Physics, Ewha Womans University, 120-750, Seoul, Korea, and Institute of Natural Sciences, Wonkwang University, Iksan, Jeonbuk, 570-749, Korea

Received December 16, 2002. Revised Manuscript Received March 25, 2003

A new quaternary compound, $AuNb_4P_2S_{20}$, was synthesized by direct solid-state reaction from Au, Nb, P, and S at 900 °C. Its structure was determined by the single-crystal X-ray diffraction method. $AuNb_4P_2S_{20}$ was dark-gray crystals with structures similar to those of ANb_2PS_{10} (A = Na, Ag). The needle-shape compound crystallizes in the monoclinic space group *C*2/*c* with cell dimensions of $a = 24.5618(10)$ Å, $b = 7.5439(11)$ Å, $c = 12.983(3)$ Å, $\beta = 92.83(2)°$, and $Z = 4$. This structure consists of one-dimensional infinite chains built by $[Nb_2S_{12}]$ and $[PS_4]$ units. Au atoms are occupied within the van der Waals gap of sulfur atoms between infinite chains to make $-S\cdots Au^{+}\cdots S-$ contacts. There is only one Au atom site and four atoms at crystallographically equivalent sites in a unit cell. This is only the half of the numbers of Na or Ag atoms in $NaNb_2PS_{10}$ or $AgNb_2PS_{10}$. The higher oxidation state, therefore, in Au or Nb should exist to make the charge neutrality. The results of XPS measurements in $AuNb_4P_2S_{20}$ indicate that there are two mixed oxidation states on Nb not on Au. Magnetic measurements suggest that the compound is antiferromagnetic material with the transition temperature of 45 K. The interrelationships between mixed oxidation states and electronic properties are discussed.

Introduction

Transition metal thiophosphates have been actively investigated because of their structural low-dimensionality and importance as oxidizing host materials for secondary lithium batteries.[1] Early transition metal thiophosphates with various phosphorus−sulfur polyanions $[P_nQ_m]^{x-}$ and low-dimensional structures have been reported. For example, V_2PS_{10} is one-dimensional,[2] and $VP_{0.2}S_2$, $VP_{0.17}S_2$, $V_2P_4S_{13}$, $V_{0.78}PS_3$, $V_2P_4S_{13}$, AVP_2S_7, Nb_2PS_{10}, $Nb_4P_2S_{21}$, and NbP_2S_8 are two-dimensional compounds.[3−9] Because the first alkali metal contained compound with $[P_nQ_m]^{x-}$ units, KNb_2PS_{10},[10] is known, we recently synthesized more family members of one-dimensional quaternary thiophosphates, ANb_2PS_{10} (A = Na, Ag).[11] The structures of ANb_2PS_{10} are closely related to that of 2D-$Nb_4P_2S_{21}$. As already known, $Nb_4P_2S_{21}$ is a two-dimensional compound where $-S-S-S-$ bridges connect neighboring one-dimensional chains. However, in ANb_2PS_{10} (A = Na, Ag, Au), the $-S-S-S-$ bridges are broken and reduced to $-S-S-$, and also instead of forming bridges between chains through A^+ cations are inserted between the chains, thereby forming $-S\cdots A^{+}\cdots S-$ contacts.

A mixed-valence compound contains an element that exhibits two distinctive oxidation states. Crystallographically, the ions having different oxidation states result in two different structures around each of them. A linear AuX_2 and a square planar AuX_4 (X = Cl, Br, I) for Au^+ and Au^{3+}, respectively, are found in Wells' cesium salts.[12−15] In most cases, such a mixed valency occurs in the compound containing transition metals. Whether the mixed valency occurs in $AuNb_4P_2S_{20}$, which contains two transition metals, or not will be interesting to investigate. Herein, the crystal structures, mixed oxidation states, electronic transport, and magnetic properties of $AuNb_4P_2S_{20}$ are discussed.

* Authors to whom correspondence should be addressed. Phone: 82-2-3277-2350. Fax: 82-2-3277-2384. E-mail: sjkim@ewha.ac.kr; or djung@wonkwang.ac.kr.

† Department of Chemistry, Ewha Womans University.

‡ Department of Physics, Ewha Womans University.

§ Institute of Natural Sciences, Wonkwang University.

(1) (a) Thompson, A. H.; Whittingham, M. S. U.S. Patent 4,049,870, 1977. (b) Brec, R.; Lemehaute, A. Fr. Patents 7,704,518 and 4,049,879, 1977. (c) Nishi, Y. *Electrochemistry* **2000**, *68*, 1008.

(2) Brec, R.; Ouvrard, G.; Evain, M.; Grenouilleau, P.; Rouxel, J. *J. Solid State Chem.* **1983**, *47*, 174.

(3) (a) Ouvrard, G.; Brec, R.; Rouxel, J. *Ann. Chim. Fr.* **1982**, *7*, 53. (b) Brec, R.; Freour, R.; Ouvrard, G.; Soubeyroux, J. L.; Rouxel, J. *Mater. Res. Bull.* **1983**, *18*, 689.

(4) Evain, M.; Brec, R.; Ouvrard, G.; Rouxel, J. *J. Solid State Chem.* **1985**, *56*, 12.

(5) Brec, R.; Grenouilleau, P.; Evain, M.; Rouxel, J. *Rev. Chim. Miner.* **1983**, *20*, 295.

(6) Brec, R.; Evain, M.; Grenouilleau, P.; Rouxel, J. *Rev. Chim. Miner.* **1983**, *20*, 283.

(7) Grenouilleau, P.; Brec, R.; Evain, M.; Rouxel, J. *Rev. Chim. Miner.* **1983**, *20*, 628.

(8) Ouvrard, G.; Freour, R.; Brec, R.; Rouxel, J. *Mater. Res. Bull.* **1985**, *20*, 1053.

(9) (a) Kopnin, E.; Coste, S.; Jobic, S.; Evain, M.; Brec, R. *Mater. Res. Bull.* **2000**, *35*, 1401. (b) Durand, E.; Evain, M.; Brec, R. *J. Solid State Chem.* **1983**, *102*, 146.

(10) Do, J.; Yun, H. *Inorg. Chem.* **1996**, *35*, 3729.

(11) Goh, E.-Y.; Kim, S.-J.; Jung, D. *J. Solid State Chem.* **2002**, *168*, 119.

(12) Kitagawa, H.; Kojima, N.; Matsushita, N.; Ban, T.; Tsujikawa, I. *J. Chem. Soc., Dalton Trans.* **1991**, 3115.

(13) Elliot, N.; Pauling, L. *J. Am. Chem. Soc.* **1938**, *60*, 1846.

(14) Brauer, G.; Sleater, G. *J. Less-Common. Met.* **1970**, *21*, 283.

(15) Ferrari, A.; Tani, E. *Gazz. Chim. Ital.* **1959**, *89*, 502.

10.1021/cm021790+ CCC: $25.00
Published on Web 05/07/2003

Table 1. Crystallographic Data for $AuNb_4P_2S_{20}$

empirical formula	$AuNb_4P_2S_{20}$
formula weight ($g \cdot mol^{-1}$)	1271.75
temperature (K)	293(2)
wavelength (Å)	0.71073
crystal system	monoclinic
space group	C_{2h}^6C2/c (No. 15)
unit cell dimensions (Å)	$a = 24.5618(10)$
	$c = 7.5439(11)$
	$c = 12.983(3)$
	$\beta = 92.83(2)°$
volume ($Å^3$)	2402.7(7)
Z	4
density (calcd)($g \cdot cm^{-3}$)	3.516
abs coeff (mm^{-1})	9.802
data/restraints/params.	2102/0/125
final R indices ($F_o^2 > 2\sigma(F_o^2)$)	R1 = 0.0282, wR2 = 0.0802
R indices ($F_o^2 > 0$, all data)	R1 = 0.0310, wR2 = 0.0846
largest diff. peak and hole ($e/Å^3$)	4.155 and −1.123

Experimental Section

Synthesis. The crystals of $AuNb_4P_2S_{20}$ were prepared from a mixture of Au powder (Kojima 99.99%), Nb powder (Kojundo 99.9%), P powder (Aldrich 99.99%), and S powder (Aldrich 99.999%) in a molar ratio of 1:2:1.1:10.3. The reacting mixture was double-sealed in an evacuated quartz tube and heated at 900 °C for 2 weeks. Then, to obtain a single crystal with size suitable for structure determination, the heated product was slowly cooled to room temperature (2 °C/h). The reactions led to the formation of shiny dark-gray needle crystals. The compound was stable in the air and moisture. Any observable evidence of side products of ternary or quaternary phases were not detected. The chemical compositions of the crystals were confirmed by an energy-dispersive X-ray (EDX) spectrometer equipped with electron probe microanalysis (EPMA; JXA-9600, EDX; LinkeXL).

Structural Analysis. Preliminary examination and data collection were performed with Mo Kα_1 radiation ($\lambda = 0.71073$ Å) on an Enraf Nonius diffractometer equipped with an incident beam monochromator graphite crystal. The unit cell parameters and an orientation matrix for data collection were obtained from the least-squares refinement, using the setting angles of 25 reflections in the range of $22° < 2\theta < 29°$. The observed Laue symmetry and systematic extinctions ($h00$, $h = 2n + 1$; $0k0$, $k = 2n + 1$; $00l$ and $h0l$, $l = 2n + 1$; $hk0$, $h + k = 2n + 1$) for the compound was indicative of the space groups C_{2h}^6C2/c and C_s^4Cc. The centrosymmetric $C2/c$ was assumed and subsequent refinements confirmed the choice of this space group.

Intensity data were collected with the ω-2θ scan technique. The intensities of three standard reflections measured every hour showed no significant deviations during the data collection. The initial positions of all atoms were obtained from the direct methods of the SHELXS-86 program.[16] The structure was refined by full-matrix least squares techniques using the SHELXL-93 program.[17] The final cycle of refinement performed on F_o^2 with 2102 unique reflections converged to residuals wR2 ($F_o^2 > 0$) = 0.0846 and the conventional R index based on the reflections having $F_o^2 > 2\sigma(F_o^2)$ was 0.0282 for $AuNb_4P_2S_{20}$. Crystallographic data for $AuNb_4P_2S_{20}$ are given in Table 1. Table 2 lists final fractional atomic coordinates and displacement parameters. Comparisons of selected bond distances and angles of $NaNb_2PS_{10}$, $AgNb_2PS_{10}$, and $AuNb_4P_2S_{20}$ are listed in Table 3.

X-ray Photoelectron Spectroscopy. XPS spectra for $AuNb_4P_2S_{20}$ and $AgNb_2PS_{10}$ had been measured with an ESCA 2000 electron spectrometer (VG microtech). Pelletized samples were mounted on an aluminum plate. Nonmonochromatic Al Kα radiation was used as an excitation source ($h\nu = 1486.6$ eV). During the measurement, the spectrometer was pumped to a residual pressure of $\sim 10^{-9}$ Torr. The data were taken from fresh samples and also after Ar bombardment on the surface of the pelletized samples. The binding energies of gold and niobium in $AuNb_4P_2S_{20}$ and $AgNb_2PS_{10}$ were measured. The 1s binding energy of carbon, 284.6 eV, was used as an internal standard.

Table 2. Atomic Coordinates ($\times 10^4$) and Equivalent Isotropic Displacement Parameters ($Å^2 \times 10^3$) for $AuNb_4P_2S_{20}$

atom	x	y	z	$U_{(eq)}$[a]
Au(1)	0	0	0	25(1)
Nb(1)	1402(1)	5664(1)	2220(1)	12(1)
Nb(2)	1409(1)	4410(1)	59(1)	13(1)
P(1)	1023(1)	1014(2)	8631(1)	15(1)
S(1)	688 (1)	6451(2)	3585(1)	14(1)
S(2)	688(1)	6277(3)	778(1)	19(1)
S(3)	2120(1)	5436(2)	3706(1)	15(1)
S(4)	1460(1)	9053(2)	2352(1)	20(1)
S(5)	9306(1)	3746(2)	3636(1)	19(1)
S(6)	1501(1)	1046(2)	9956(1)	20(1)
S(7)	8425(1)	3357(2)	1364(1)	16(1)
S(8)	7891(1)	3622(3)	9015(1)	20(1)
S(9)	2119(1)	3795(4)	1422(2)	19(1)
S(10)	9542(1)	934(3)	1408(1)	23(1)

[a] $U_{(eq)}$ is defined as one-third of the trace of the orthogonalized U_{ij} tensor.

Table 3. Selected Bond Distances (Å) and Bond Angles (deg) for $NaNb_2PS_{10}$, $AgNb_2PS_{10}$, and $AuNb_4P_2S_{20}$

	$NaNb_2PS_{10}$	$AgNb_2PS_{10}$	$AuNb_4P_2S_{20}$
Nb−S	2.464(2)−2.666(2)	2.455(3)−2.656 (3)	2.466(2)−2.624(2)
Nb−Nb	2.891(1)−3.757(1)	2.870(2)−3.756(2)	2.961(1)−3.686(1)
P−S	1.988(3)−2.071(3)	1.987(5)−2.064(4)	2.019(3)−2.081(3)
S−S	2.017(3)−2.053(2)	2.022(5)−2.056(4)	2.029(3)−2.061(2)
A−S	2.801(4)−4.209(7)	2.544(8)−4.319(5)	2.305(2)−3.774(2)

Table 4. Atomic Orbital Parameters Used in Extended Hückel Calculations

atom	orbital	H_{ii} (eV)[a]	ζ_1	C_1	ζ_2	C_2
S	3s	−20.0	2.122	1.0		
	3p	−13.3	1.827	1.0		
P	3s	−18.6	1.75	1.0		
	3p	−14.0	1.30	1.0		
Nb	5s	−10.1	1.89	1.0		
	5p	−6.86	1.85	1.0		
	4d	−12.1	4.08	0.6401	1.64	0.5516
Au	6s	−10.92	2.602	1.0		
	6p	−5.55	2.584	1.0		
	5d	−15.076	6.163	0.64418	2.791	0.53558

[a] $H_{ii} = \langle\chi_i|H^{eff}|\chi_i\rangle$, $i = 1,2,3,....$ The value approximated by valence-state ionization potential.

Electronic Structure Calculation. Electronic structure calculations for $AuNb_4P_2S_{20}$ were performed by the extended Hückel method within the framework of tight-binding approximation.[18] Density of states (DOS) were calculated based on the given crystal structure for 396 k-points. The atomic orbital parameters employed in the calculation were the default values in the CAESAR program,[19] which are listed in Table 4.

Electron Transport Measurements. The electrical resistance of a single-crystalline $AuNb_4P_2S_{20}$ was measured using the four-probe method over the temperature range 80−300 K. Four 20-μm wires were connected to the sample by silver paste. A low-frequency lock-in technique was adopted to measure the resistivity.

Magnetic Susceptibility Measurements. Magnetic susceptibility data were recorded on a MPMS5 magnetometer (Quantum Design Inc.). The calibration was made at 298 K

(16) Sheldrick, G. M. *Acta Crystallogr.* **1990**, *A46*, 467.
(17) Sheldrick, G. M. SHELXL 93, Program for the Refinement of Crystal Structures; University of Göttingen: Germany, 1993.
(18) Hoffman, R. *J. Chem. Phys.* **1963**, *39*, 1397.
(19) Ren, J.; Liang, W.; Whangbo, M.-H. CAESAR; Primecolor Software, Inc.: Cary, NC, 1999.

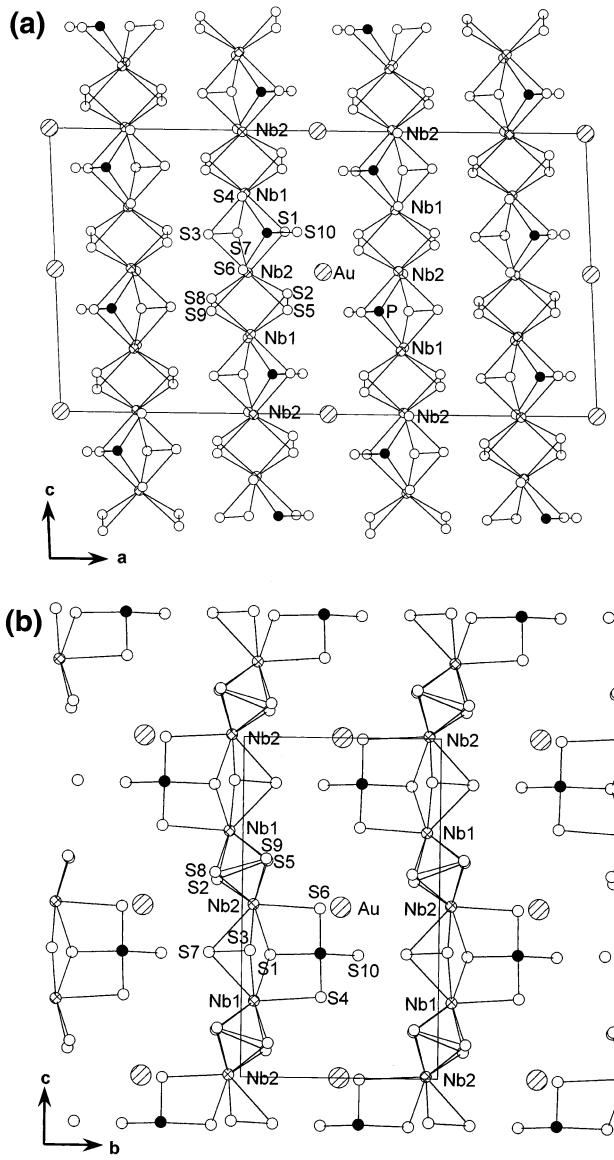

Figure 1. (a) Crystal structure of $AuNb_4P_2S_{20}$ projected along the *b*-axis, where $^1_\infty[\ [Nb_2PS_{10}^-]$ chains and a unit cell are shown. (b) Side view of one row of the stacked chains in (a). Small open circles are S atoms, small solid circles are P atoms, small cross-hatched circles are Nb atoms, and large cross-hatched circles are Au atoms.

using a palladium reference sample furnished by Quantum Design Inc. The data were collected over a temperature range of 15−300 K at a magnetic field of 5000 G and were corrected for diamagnetism.

Results and Discussion

Crystal Structure. The structure of quaternary thiophosphates $AuNb_4P_2S_{20}$ is similar to those of the ANb_2PS_{10} (A = Na, Ag) family except for cation positions within a one-dimensional chain framework. Figure 1(a) shows the crystal structure of $AuNb_4P_2S_{20}$, which is projected on the *ac*-plane. In Figure 1(b), a side view of one row of the stacked chains of Figure 1(a) is shown. The building blocks of the chains are constructed with $[Nb_2S_{12}]$ and $[PS_4]$ units. In $[Nb_2S_{12}]$, each Nb atom is centered in a distorted bicapped trigonal prism composed of three S_2^{2-} anions. The bond distances between S and S in the S_2^{2-} anion are in the range of 2.029(3)−2.061(2) Å, which is typical for the S_2^{2-} dimer anion. The $[PS_4]$ units are attached to make bridges between two $[Nb_2S_{12}]$ units to make the long Nb−Nb pair. (The short Nb−Nb interactions are found in the $[Nb_2S_{12}]$ unit itself). Accordingly, the short and long Nb−Nb interactions originate from whether or not there is a $[PS_4]$ unit between the metals.

Scheme 1

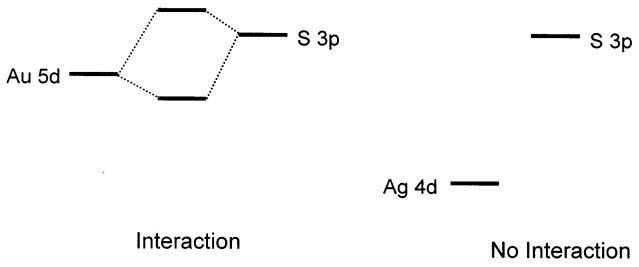

Au atoms in $AuNb_4P_2S_{20}$ are located in sites that are slightly different from those of Na^+ and Ag^+ cations in $NaNb_2PS_{10}$ and $AgNb_2PS_{10}$. Au atoms are occupied on a special position in $AuNb_4P_2S_{20}$ crystal with inversion symmetry, however, Na^+ and Ag^+ cations are occupied in the general positions in $NaNb_2PS_{10}$ and $AgNb_2PS_{10}$. As shown in Figure 1(b), Au atoms are filled to make Au−S contacts near the $[PS_4]$ units between Nb(2) atoms of two neighboring chains. However, in $NaNb_2PS_{10}$ and $AgNb_2PS_{10}$, A−S (A = Na, Ag) is located between the two short Nb−Nb pairs and $[PS_4]$ units of two neighboring chains. Na^+ and Ag^+ cations in $NaNb_2PS_{10}$ and $AgNb_2PS_{10}$ reside in exactly the same sites in the van der Waals gap between infinite chains making nine Na−S and Ag−S interactions at 2.801(4)−4.209(7) Å and at 2.544(8)−4.319(5) Å, respectively. Au atoms in $AuNb_4P_2S_{20}$ are in close contact with S atoms in the range of 2.305(2)−3.774(2) Å. The results of the A−S (A = Na, Ag, Au) bond distances are exactly inverse of the cation sizes (see the radii of 116, 129, and 151 pm for Na^+, Ag^+, and Au^+, respectively, when the coordination number is six). An Au atom can make a strong covalent interaction with S atoms because the energy level of its d orbital lies close to that of the S p orbital, whereas the interaction should be weak for an Ag atom because of the large energy difference, as briefly shown in Scheme 1. The shortest Au−S(10) contacts at 2.305(2) Å are very close to the lengths of the linear Au−S contacts found in KAuS, $KAuS_5$, and Na_3AuS_2.[20−22]

The short and long Nb−Nb distances along the chain direction are 2.961(1) Å and 3.686(1) Å, respectively, which are similar to the distances found in ANb_2PS_{10} and in other ternary compounds Nb_2PS_{10} and $Nb_4P_2S_{21}$. The Nb−S distances are in the range of 2.466(2)−2.624(2) Å with the average bond length of 2.538(2) Å in $AuNb_4P_2S_{20}$. The average distance of P−S bonds is 2.040(3) Å, which is similar to that of $AgNb_2PS_{10}$. There is no notable feature in the Nb−S bond lengths; within error range, Nb−S bond lengths are almost the same. In the long run, the different aspects between $AuNb_4P_2S_{20}$ and ANb_2PS_{10} (A = Na, Ag) are the cation−sulfur distance and the number of cations.

(20) Klepp, K. O.; Bronger, W. *J. Less-Common Met.* **1987**, *128*, 65.
(21) Klepp, K. O.; Weithaler, C. *Z. Kristallogr.* **1998**, *213*, 18.
(22) Klepp, K. O.; Bronger, W. *J. Less-Common Met.* **1987**, *132*, 173.

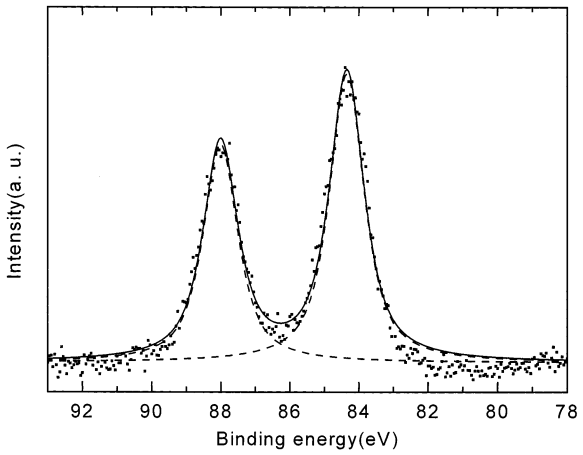

Figure 2. Au 4f X-ray photoelectron spectrum for $AuNb_4P_2S_{20}$. The dashed lines are the fitted $4f_{5/2}$ and $4f_{7/2}$ curves of Au^+, and the solid line is the sum of the two fitted curves.

Table 5. Results of Curve Fit to Au 4d Spectrum of $AuNb_4P_2S_{20}$

binding energy (eV)	fwhm (eV)	area (%)	state
84.4	1.20	57.0	$4f_{7/2}$ (Au^+)
88.0	1.20	43.0	$4f_{5/2}$ (Au^+)

Table 6. Results of Curve Fit to Nb 3d Spectrum of $AgNb_2P_2S_{10}$

binding energy (eV)	fwhm (eV)	area (%)	state
203.4	1.17	59.9	$3d_{5/2}$ (Nb^{4+})
206.2	1.17	40.1	$3d_{3/2}$ (Nb^{4+})

Table 7. Results of Curve Fit to Nb 3d Spectrum of $AuNb_4P_2S_{20}$

binding energy (eV)	fwhm (eV)	area (%)	state
203.5	1.14	41.1	$3d_{5/2}$ (Nb^{4+})
206.2	1.14	29.1	$3d_{3/2}$ (Nb^{4+})
207.6	1.15	18.5	$3d_{5/2}$ (Nb^{5+})
210.3	1.15	11.2	$3d_{3/2}$ (Nb^{5+})

The stoichiometry of $AuNb_4P_2S_{20}$ instead of $AuNb_2PS_{10}$ suggests that there might be some higher oxidation states on the Au atom or other elements such as Nb atoms. Several Au compounds have been known to show mixed valence states $Au^{3+}(d^8)$ and $Au^+(d^{10})$. The geometry for Au^{3+} is square planar, whereas that for Au^+ is linear. Because there is only one crystallographical position on Au with linear S−Au−S structure in $AuNb_4P_2S_{20}$, the possibility of mixed valence states on Au is excluded. Instead, there might be some mixed valence states on Nb atoms to compensate for the positive charge in the compound, as there are two distinctively different Nb sites. Consequently, the $(Au^{1+})[(Nb_2S_6)_2]^{5+}(PS_4^{3-})_2$ scheme seems to be a reasonable suggestion to satisfy the charge neutrality.

XPS Spectra. XPS experiments were carried out to examine the oxidation states of Au and Nb in $AuNb_4P_2S_{20}$ and the results are listed in Tables 5, 6, and 7. The binding energies at 84.4 and 88.0 eV are typical indications for Au $4f_{7/2}$ and $4f_{5/2}$, respectively, when the Au is monopositive.[23] (see Figure 2). Any indication of Au^{3+}, whose peak is typically shown at >90 eV is not found. In the long run all Au in $AuNb_4P_2S_{20}$ can be assigned to be Au^+. Figures 3 and 4 show Nb 3d level XPS spectra

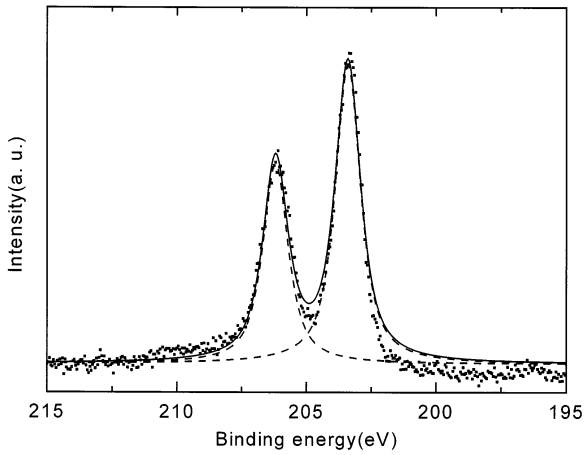

Figure 3. Nb 3d X-ray photoelectron spectrum for $AuNb_4P_2S_{20}$. The dashed lines are the fitted $3d_{3/2}$ and $3d_{5/2}$ curves of Nb^{4+}, and the solid line is the sum of the two fitted curves.

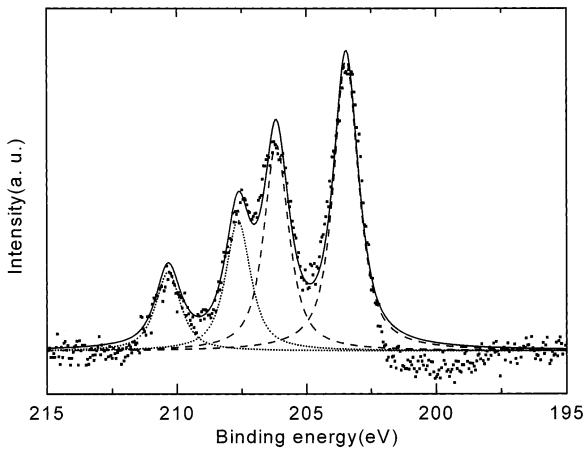

Figure 4. Nb 3d X-ray photoelectron spectrum for $AuNb_4P_2S_{20}$. The dashed lines are the fitted $3d_{3/2}$ and $3d_{5/2}$ curves of Nb^{4+}, the dotted lines are those of $Nb^{4+\delta}$, and the solid line is the sum of the four fitted curves.

of $AgNb_2PS_{10}$ and $AuNb_4P_2S_{20}$, respectively. The Nb 3d level XPS spectrum of $AgNb_2PS_{10}$ shows doublets at 203.4 and 206.2 eV indicating Nb^{4+}.[24] The XPS data of $AuNb_4P_2S_{20}$ shows three peaks indicating more than one Nb oxidation state. Because there are two crystallographically different Nb atoms, the oxidation states of the two Nb atoms can be different. The three peaks could be resolved into two pairs of Nb $3d_{3/2}$ and $3d_{5/2}$. The first doublet at 207.6 and 210.3 eV which is left-shifted is assigned to Nb^{5+} and the second doublet appears at the similar binding energy of $AgNb_2PS_{10}$ at 203.5 and 206.2 eV, therefore, it is assigned to Nb^{4+}.

Electronic Structure. Projected density of states (PDOS) calculated for $AuNb_4P_2S_{20}$ are shown in Figure 5. PDOS data support the existence of mixed valence not in Au but in Nb. All Au 5d orbital lies well below the Fermi level, but Nb 4d orbital lies below and above the Fermi level, which means that the oxidation states of Au and Nb are +1, and +(4+α), respectively. Rather strong interaction of Au−S is supposed to be the reason the charge transfer occurs from Nb to Au through the

(23) Szytula, A.; Penc, F. B.; Jezierski, A. *J. Alloys Compd.* **2001**, *317−318*, 340.

(24) (a) Bahl, M. K. *J. Phys. Chem. Solids* **1975**, *36*, 485. (b) Kim, S.-J.; Bae, H.-S.; Yee, K.-A.; Choy, J.-H.; Kim, D.-K.; Hur, N.-H. *J. Solid State Chem.* **1995**, *115*, 427. (c) McGuire, G. E.; Schweitzer, G. K.; Carlson, T. A. *Inorg. Chem.* **1973**, *12*, 2450.

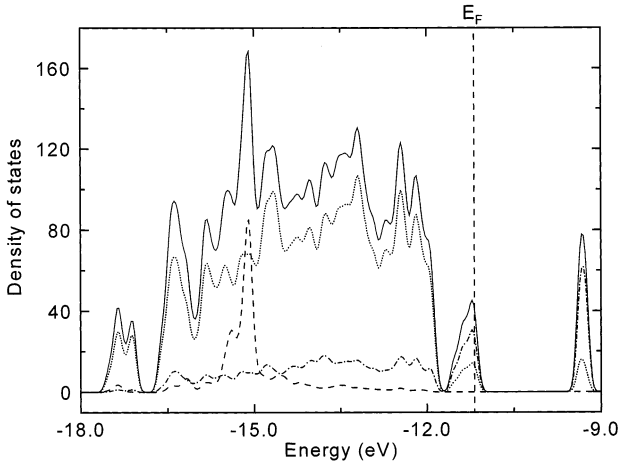

Figure 5. Projected density of states (PDOS) curves calculated for $AuNb_4P_2S_{20}$. The solid line, the dotted line, the dash−dotted line, and the dashed line represent the total DOS, the PDOS of the S 3p, the PDOS of the Nb 4d, and the PDOS of the Au 5d orbitals, respectively.

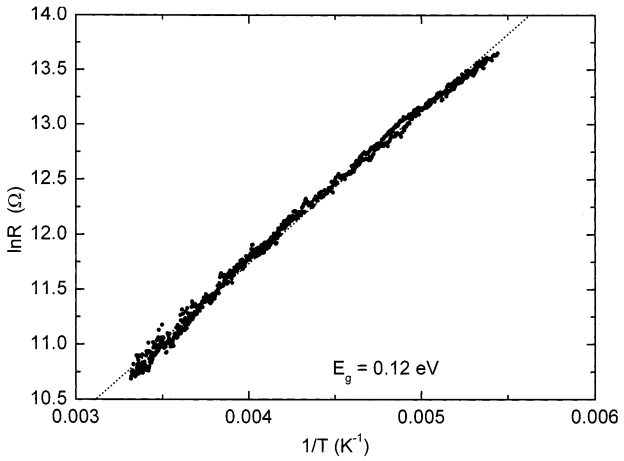

Figure 6. Temperature dependence of electrical resistivity for a single crystal of $AuNb_4P_2S_{20}$.

Nb−S−Au contact. Electrons move from Nb 4d to Au 5d because the energy level of Nb 4d is higher than that of Au 5d. Consequently, the mixed valency occurs on Nb (i.e., Nb^{4+} and Nb^{5+}) but not on Au (i.e., Au^{+}). This result is consistent with the XPS and crystallographical data. Both valence sums for the two Nb sites and the partial DOS values for the d orbitals of Nb atoms in Figure 1 suggest that Nb(1) and Nb(2) slightly favor Nb^{4+} and Nb^{5+} states, respectively.

Electron Transport and Magnetic Properties. The temperature dependency of the electrical resistivity for $AuNb_4P_2S_{20}$ is shown in Figure 6. $AuNb_4P_2S_{20}$ showed semiconducting behavior; the band gap is 0.11 eV with resistivity of 1.4×10^2 Ωcm at room temperature. The resistivity of $AuNb_4P_2S_{20}$ is much lower than those of ANb_2PS_{10} (A = Na, Ag); the resistivities of these compounds were larger than 50 KΩcm. The band gap of $NaNb_2PS_{10}$ and $AgNb_2PS_{10}$ were 0.28 and 0.16 eV, respectively. The result of DOS calculated for $AuNb_4P_2S_{20}$ shows that the compound is metallic because of the shortage of electrons donated by the cation (i.e., see the stoichiometries of $AuNb_4P_2S_{20}$ and $AgNb_2PS_{10}$). In the metallic figure, the valence band of $AuNb_4P_2S_{20}$ consists of mainly Nb d orbital with the d^1 or d^0 electronic configuration according to the mixed valency on Nb. It

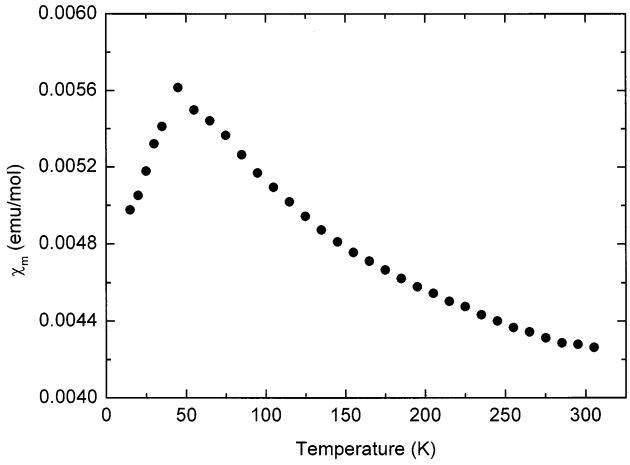

Figure 7. Plots of molar magnetic susceptibility (χ_m, emu/mol) vs temperature (K) for $AuNb_4P_2S_{20}$.

Scheme 2

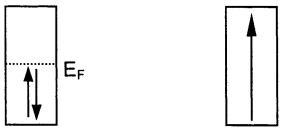

is well established that the electronic state of a crystalline solid with a partially filled band may not become metallic but insulating so as to minimize electron−electron repulsion (see Scheme 2).[25] Such an insulating state can be magnetic or nonmagnetic depending upon how electron−electron repulsion is minimized. For instance, a magnetic insulating state of the Slater antiferromagnetism introduces spin density alternation at neighboring sites, thus decreasing the on-site electron−electron repulsion. To understand the difference between the results of electronic structure calculation and electron transport measurement, magnetic measurements were performed. The discrepancy between the calculated and experimental results suggests that the compound might be a magnetic insulator. The magnetic susceptibility data in Figure 7 clearly show that $AuNb_4P_2S_{20}$ illustrates ferromagnetic and antiferromagnetic properties with the transition temperature of 45 K.

Conclusions

The new quaternary compound $AuNb_4P_2S_{20}$ was prepared and characterized. Because the compound contains fewer cations in a unit cell, the role of Nb in $AuNb_4P_2S_{20}$ is quite different from that of the already known compounds ANb_2PS_{10}(A = Na, Ag). The oxidation states of A and Nb in ANb_2PS_{10} (A = Na, Ag) are +1 and +4, respectively. However, partial amounts of Au or Nb should have higher oxidation states to balance the charge in $AuNb_4P_2S_{20}$. The mixed valencies such as Au^{1+} and Au^{3+}, or Nb^{4+} and Nb^{5+}, are, therefore, expected. The XPS data tell us that the mixed valence state arises on Nb atoms not on Au atoms only in $AuNb_4P_2S_{20}$, which is not found in ANb_2PS_{10} (A = Na, Ag). This conclusion is consistent with the results of the crystal structure of Au environment and projected

(25) Canadell, E.; Whangbo, M.-H. *Chem. Rev.* **1991**, *91*, 956.

density of states (PDOS) data. The discrepancy between the calculated and resistivity measurements suggest that the compound might be a magnetic insulator. The magnetic susceptibility data clearly show that $AuNb_4P_2S_{20}$ has antiferromagnetic transition at ~45 K.

Acknowledgment. S.-J. Kim acknowledges financial support from the Basic Research Program of the Korean Science & Engineering Foundation (2000-1-12200-002-3). D. Jung acknowledges financial support from the Korean Science & Engineering Foundation with Grant R02-2000-00067.

Supporting Information Available: Tables of crystal data, structure solution and refinement, atomic coordinates, bond lengths and angles, and anisotropic thermal parameters, as well as structure factors, for $AuNb_4P_2S_{20}$ (PDF). This material is available free of charge via the Internet at http://pubs.acs.org.

CM021790+